arXiv:1301.1488v2 [cond-mat.str-el] 19 Nov 2013

Detect Spinons via Spin Transport

Chui-Zhen Chen,[1] Qing-feng Sun,[1] Fa Wang,[2] and X. C. Xie[2]
[1] *Institute of Physics, Chinese Academy of Sciences, Beijing 100190, China*
[2]*International Center for Quantum Materials and School of Physics, Peking University, Beijing 100871, China*
(Dated: December 16, 2013)

Existence of spinons is the defining property of quantum spin liquids. These exotic excitations have (fractionalized) spin quantum number and no electric charge, and have been proposed to form Fermi surfaces in the recently discovered organic spin liquid candidates. However direct probes for them are still lacking. In this paper we propose to experimentally identify the spinons by measuring the spin current flowing through the spin liquid candidate materials, which would be a direct test for the existence of spin-carrying mobile excitations. By the nonequilibrium Green function technique we evaluate the spin current through the interface between a Mott insulator and a metal under a spin bias, and find that different kinds of Mott insulators, including quantum spin liquids, can be distinguished by different relations between the spin bias and spin current, In the end we will also discuss relations to experiments and estimate experimentally relevant parameters.

PACS numbers: 75.10.Jm,72.25.Mk,73.23.-b, 73.40.Rw

Quantum spin liquid(QSL) was first proposed by Anderson as an alternative ground state against long range magnetic order in frustrated magnets[1]. In these systems competing spin exchange interactions result in a large degeneracy of classical ground states, and quantum fluctuations among these states destroy long range symmetry breaking order.[2] A particular kind of quantum spin liquid, the resonant valence bond(RVB) state, has also been proposed to be the key to the high-temperature superconductivity in the cuprate materials.[3,4]After decades of intense research many numerical evidences of QSL ground states have been found in semi-realistic lattice models[5–15], and many artifical parent Hamiltonians for spin liquids have been constructed[16–18].

On the other hand, the experimental realization of spin liquids in more than one spatial dimensions remains challenging until several candidate materials have been discovered recently.[2,19] Two two-dimensional(2D) triangle lattice organic salts $\mathrm{EtMe_3Sb[Pd(dmit)_2]_2}$ and κ-$\mathrm{(BEDT\text{-}TTF)_2Cu_2(CN)_3}$, the kagome lattice herbertsmithite $\mathrm{ZnCu_3(OH)_6Cl_2}$ and a three-dimensional hyperkagome lattice $\mathrm{Na_4Ir_3O_8}$ are found to be the most promising candidates of QSL.[20–23] Despite of structural distinction, they are all Mott insulators with competing interactions and show no magnetic order down to much lower temperature than their exchange interaction. Current measurements of magnetic susceptibility, specific heat, thermal transport and neutron scattering have provided vital information about the properties of these materials.[24–27] However, there is still no definitive experiment for the identification of quantum spin liquids.[2]

One of the most significant features of quantum spin liquids is that they have exotic excitations called spinons which are uncharged and usually spin-1/2 mobile particles, may obey bosonic or fermionic statistics and may have a gap or not.[2,19] The fermionic spinons may form Fermi surfaces and are generally accompanied by an emergent gauge field.[28,29] This “spinon Fermi sea” state has received strong support from the observations of metallic-like specific heat and thermal conductivity[30] in the organic candidates at low temperatures. However these experiments do not provide a direct proof that the mobile and possibly fermionic low energy excitations are spinons. A more reliable proof for the spinon Fermi sea would be the metallic-like spin transport in these Mott insulators.

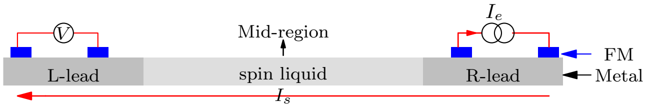

FIG. 1: (Color online). Schematic plot of a four-terminal device for the detection of spin current through a spin liquid. Four small blue bars indicate ferromagnetic electrodes. A spin polarized current is injected into the right lead(R-lead) by a current source(I_e), thus creates a spin bias and drives a spin current through the spin liquid middle region. The spin bias induced by the spin current in the left lead(L-lead) is then measured by a voltmeter(V). We will also consider other kinds of Mott insulators as the middel region instead of spin liquids.

In this paper, we propose a four-terminal measurement of spin current through a spin liquid material (Mott insulator) as the evidence for the existence of spinons. The proposed four-terminal device consists of a spin liquid material coupled to the left and right normal metal leads and each lead couples to two ferromagnetic(FM) electrodes as shown in Fig. 1.[31] A current source is added between the two right FM electrodes. This is used to create a spin polarized current flowing from one right FM electrode through the right lead to another right FM electrode, leading to a spin-solved chemical potential (i.e. a spin bias V_R) in the right lead. Then this spin bias will drive a spin current flowing from the right lead through the spin liquid and finally into the left lead by the spinon-electron spin-exchange interaction at the interfaces between the spin liquid and the leads. At last, a voltmeter is connected to the two left FM electrodes which are in contact to the left lead. The voltmeter is used to measure the spin bias V_L created by the spin current in the left lead. Here, the spin bias V_α ($\alpha = L, R$) is defined as the difference between the spin-↑ chemical potential $\mu_{\alpha\uparrow}$ and the spin-↓ chemical potential $\mu_{\alpha\downarrow}$ in the α-lead, i.e. $V_\alpha \equiv \mu_{\alpha\uparrow} - \mu_{\alpha\downarrow}$.[32,33]

In the rest of this paper, we will first establish the general result of the spin current through the interface between a Mott insulator in the middle region and a metallic right lead with a spin bias (see Fig. 1) by the nonequilibrium Green function technique. We will then apply the general formalism to show that different Mott insulators can be distinguished by different relations between the spin current and the spin bias as well as temperature. In the end we will also discuss relations to experiments and estimate experimentally relevant parameters.

The model Hamiltonian and formulation. In our theoretic analysis, we consider the model of a Mott insulator (a spin liquid or a collinear antiferromagnet) coupled to two normal leads under a spin bias on the right lead. The Hamiltonian of the system is given by $H = H_0 + H_M + H_I$, where H_0, H_M, and H_I are the Hamiltonians of the leads (Metal), the middle region (Mott insulator), and the interfaces respectively. H_0 and H_I are assumed to be

$$H_0 = \sum_{\alpha=L,R} \sum_{\boldsymbol{k},\sigma} \xi_{\alpha k\sigma} c^\dagger_{\alpha \boldsymbol{k}\sigma} c_{\alpha \boldsymbol{k}\sigma}, \tag{1}$$

and

$$H_I = J_I \sum_{\boldsymbol{r_0}} \boldsymbol{S}_R(\boldsymbol{r_0}) \cdot \boldsymbol{S}_M(\boldsymbol{r_0}) + J_I \sum_{\boldsymbol{r_1}} \boldsymbol{S}_L(\boldsymbol{r_1}) \cdot \boldsymbol{S}_M(\boldsymbol{r_1}), \tag{2}$$

where

$$\boldsymbol{S}_\alpha(\boldsymbol{r}) = \frac{1}{2} \sum_{\mu,\mu'} \boldsymbol{\sigma}_{\mu\mu'} c^\dagger_{\alpha\mu}(\boldsymbol{r}) c_{\alpha\mu'}(\boldsymbol{r}),$$

with $\boldsymbol{S}_M(\boldsymbol{r})$ the (dimensionless) spin operator of the middle region at the position $\boldsymbol{r}$. $c_{\alpha\boldsymbol{k}\sigma}(c^\dagger_{\alpha\boldsymbol{k}\sigma})$ is creation (annihilation) of the spin-σ electron in the α=(L,R)-lead. $\xi_{\alpha k\sigma} = \varepsilon_{\alpha k} - \mu_{\alpha\sigma}$, where $\varepsilon_{\alpha\boldsymbol{k}}$ is the electron dispersion relation and $\mu_{\alpha\sigma=(\uparrow,\downarrow)}$ is the spin dependent chemical potential in the α-lead. The spin exchange interaction constants J_I is determined by the interface properties of Mott insulator and metal.[34] $\sum_{\boldsymbol{r_0}}$ means integral over the interface. H_M depends on the type of the Mott insulator we consider and will be specified later. We emphasize that there is *no* single electron tunneling term in H_I because the middle region is a Mott insulator.

Due to the spin exchange interaction in H_I, the spin current can flow from the normal lead to Mott insulator and vice versa. When the right lead is under a spin bias, the spin current I_s flowing into the middle region from the right lead is,

$$\begin{aligned} I_s &= -< \frac{d}{dt} \boldsymbol{S}^z_T >= i < [\boldsymbol{S}^z_T, H(t)] > \\ &= i\, J_I \sum_{\boldsymbol{r}_0} < [\boldsymbol{S}^z_T, \boldsymbol{S}_R(\boldsymbol{r_0}) \cdot \boldsymbol{S}_M(\boldsymbol{r_0})] > \\ &= J_I \sum_{\boldsymbol{r}_0} Re(\Gamma^<(\boldsymbol{r}_0, t, t)), \end{aligned} \tag{3}$$

with $\boldsymbol{S}^z_T \equiv (\hbar/2)(N_\uparrow - N_\downarrow) = (\hbar/2)\sum_{\boldsymbol{k}}(c^\dagger_{R\boldsymbol{k}\uparrow} c_{R\boldsymbol{k}\uparrow} - c^\dagger_{R\boldsymbol{k}\downarrow} c_{R\boldsymbol{k}\downarrow})$. Here, we have used the fact that $[\boldsymbol{S}^z_T, H_0] = 0$ and defined $\Gamma^<(\boldsymbol{r}_0, t, t) = i < S^-_M(\boldsymbol{r}_0, t) c^\dagger_{R\uparrow}(\boldsymbol{r}_0, t^)\} c_{R\downarrow}(\boldsymbol{r}_0, t) >$ with $S^-_M(\boldsymbol{r}_0) = S^x_M(\boldsymbol{r}_0) - iS^y_M(\boldsymbol{r}_0)$.

In order to solve the Keldysh Green functions above, we first apply equation of motion technique to solve $\Gamma^t(\boldsymbol{r}_0, \boldsymbol{k}, \boldsymbol{k}', \tau, \tau') = -i < T_c\{S^-_M(\boldsymbol{r}_0, \tau) c_{R\boldsymbol{k}\downarrow}(\tau) c^\dagger_{R\boldsymbol{k}'\uparrow}(\tau')\} >$,[35,36]

By keeping the lowest order terms of J_I we have

$$\begin{aligned} &\Gamma^t(\boldsymbol{r}_0, \boldsymbol{k}, \boldsymbol{k}', \tau, \tau') \\ &= \frac{-iJ_I}{2N_R} \sum_{\boldsymbol{r}_0} \int d\tau_1 \chi^t(\boldsymbol{r}_0, \boldsymbol{r}'_0, \tau, \tau_1) g^t_{R\downarrow}(\boldsymbol{k}, \tau, \tau_1) \\ &\quad \times g^t_{R\uparrow}(\boldsymbol{k}', \tau_1, \tau') \exp[-i(\boldsymbol{k} - \boldsymbol{k}') \cdot \boldsymbol{r}_0], \end{aligned}$$

where $\chi^t(\boldsymbol{r}_0, \boldsymbol{r}'_0, \tau, \tau_1) = -i < T_c[S^-_M(\boldsymbol{r}_0, \tau) S^+_M(\boldsymbol{r}'_0, \tau_1)] >$ and $g^t_{R\sigma}(\boldsymbol{k}', \tau, \tau') = -i < T_c[c_{R\boldsymbol{k}'\sigma}(\tau) c^\dagger_{R\boldsymbol{k}'\sigma}(\tau')] >$ are contour-order Green functions for spin operator in middle region and free electrons in right lead, respectively. $\Gamma^<(\boldsymbol{r}_0, \boldsymbol{k}, \boldsymbol{k}', t, t') = i < S^-_M(\boldsymbol{r}_0, t) c^\dagger_{R\boldsymbol{k}'\uparrow}(t') c_{R\boldsymbol{k}\downarrow}(t) >$ can be obtained by analytic continuation from Γ^t, and a Fourier transform then produces $\Gamma^<(\boldsymbol{r}_0, t, t)$. Plug the result into Eq. (3) we have

$$\begin{aligned} I_s &= \frac{J_I^2 N_\perp}{4N_R^2 N_M^2} \sum_{\boldsymbol{q},\boldsymbol{k},\boldsymbol{k}'} A_M(\boldsymbol{q}, \xi_{Rk'\uparrow} - \xi_{Rk\downarrow} + V) \delta_{\boldsymbol{q}_\perp + \boldsymbol{k}_\perp - \boldsymbol{k}'_\perp} \\ &\quad \times \{[1 + n_B(\xi_{Rk'\uparrow} - \xi_{Rk\downarrow} + V)] n_F(-\xi_{Rk\downarrow}) n_F(\xi_{Rk'\uparrow}) \\ &\quad - n_B(\xi_{Rk'\uparrow} - \xi_{Rk\downarrow} + V) n_F(\xi_{Rk\downarrow}) n_F(-\xi_{Rk'\uparrow})\} \end{aligned} \tag{4}$$

where N_M and N_R are the number of unit cells in the middle region and right lead, respectively. Here $N_\perp$ is the number of transverse mode(parallel to the interface) and $V = \mu_{R\uparrow} - \mu_{R\downarrow}$ is the spin bias in the right lead. $n_B(\omega)$ and $n_F(\xi_{Rk\sigma})$ are the Bose and Fermi distribution functions, respectively. $\delta_{\boldsymbol{q}_\perp + \boldsymbol{k}_\perp - \boldsymbol{k}'_\perp}$ indicates transverse(parallel to the interface) momentum conservation. The power spectrums A_M are defined as $A_M(\boldsymbol{q}, \omega) = \int dt < S^-_M(-\boldsymbol{q}, t) S^+_M(\boldsymbol{q}, 0) > \exp(i\omega t)/n_B(\omega)$, where $S^\pm_M(\boldsymbol{q}, t)$ is the Fourier transform of $S^\pm_M(\boldsymbol{r}, t) = S^x_M(\boldsymbol{r}, t) \pm S^y_M(\boldsymbol{r}, t)$.

We note that the behavior of the spin current is mainly determined by the power spectrum A_M of the middle region. Under appropriate conditions the momentum integrations over $\boldsymbol{q}, \boldsymbol{k}, \boldsymbol{k}'$ can be approximately separated, and the transverse momentum conservation factor $\delta_{\boldsymbol{q}_\perp + \boldsymbol{k}_\perp - \boldsymbol{k}'_\perp}$ will provide only a constant factor[37]. The

Fermi (Bose) function will be treated exactly at zero temperature and expanded in series of $V/(k_BT)$ at finite temperature. In the following parts of this paper we will apply Eq. (4) and analyze several kinds of Mott insulators as the middle region, including several spin liquids.

Spin liquids. Spinons in spin liquids may or may not be gapped. The gapped spin liquids will have exponentially vanishing spin transport at low temperature and small spin bias. We therefore restrict ourselves to the type of QSLs with gapless fermionic spinons. We describe such spin liquids by the following mean-field Hamiltonian

$$H_M = \sum_{\boldsymbol{k},\sigma} \zeta_k f^\dagger_{\boldsymbol{k}\sigma} f_{\boldsymbol{k}\sigma},$$

where f are fermionic spinons and $\zeta_k = \epsilon_k - \mu_s$ with μ_s the spinon chemical potential. The spinon dispersion ϵ_k may have a Fermi surface (the "spinon Fermi sea" state[28,29]) or Dirac points at Fermi level[38].

For illustration purpose we first consider a one-dimensional(1D) spinon Fermi sea state. In 1D case the transverse momentum conservation factor in Eq. (4) does not exist, and the momentum integrations can be done separately. At $T = 0$ and $\mu_s >> \omega$, since $\epsilon_q = \hbar^2 q^2/(2m_s)$ with m_s the spinon effective mass, the power spectrum A_M divided by N_R^2 and integrated over momentum q (the "density of states of spin excitations") is

$$\frac{1}{N_R^2}\sum_q A_M(q,\omega) \propto \omega.$$

Replace it in Eq.4, we find spin current $I_s \propto V^3$ at $T = 0$, and $I_s \propto (k_BT)^2 V$ at $T > 0$ with $V << k_BT$.

Now we come to the two dimensional spinon Fermi sea case, which is the most relevant to the 2D organic spin liquid candidate materials.

The spinon dispersion is $\epsilon_q = \hbar^2 q^2/(2m_s)$ with m_s the spinon effective mass, the density of states of spin excitations is

$$\frac{1}{N_R^2}\sum_{\boldsymbol{q}} A_M(q,\omega) \;=\; 2\pi N_s^2(E_F^s)\omega \propto \omega.$$

Thus the spin current $I_s \propto V^3$ at $T = 0$ (see Fig.2), and $I_s \propto (k_BT)^2 V$ at $T > 0$ with $V << k_BT$ (see Fig.3).

In the two dimensional Dirac spin liquid case[38], the low energy spinon dispersion is $\epsilon_q = \pm\hbar v_F|q - q_F|$, with v_F the Fermi velocity and q_F the Fermi vector.

At T=0, since $\sum_{\boldsymbol{q}} A_M(q,\omega)/N_R^2 \propto \omega^3$, the spin current $I_s \propto V^5$. At $T > 0$, $V << k_BT$, expanding I_s in the series of $V/(k_BT)$ directly, we find $I_s \propto (k_BT)^4 V$.

Collinear antiferromagnetic Néel order. Antiferromagnetic(AFM) order is a common competitor for quantum spin liquids. Let us now consider the simplest AFM ordered state, the collinear AFM Néel order on a bipartite lattice, and show that it has different spin transport behavior compared to the previous spin liquid cases. We describe the spin excitations by a linearized spin wave Hamiltonian,

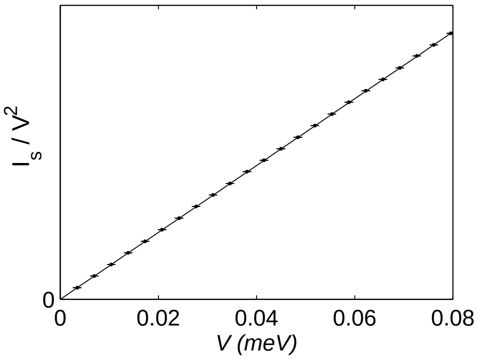

FIG. 2: (Color online) In 2D spinon Fermi sea case, the scattered dots are the spin bias V dependence of I_s/V^2 at zero temperature (fitted by simple line). The cut point at origin directly indicates $I_s \propto V^3$.

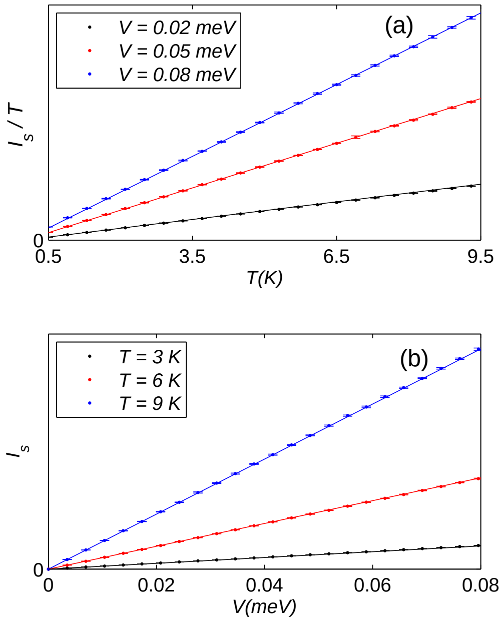

FIG. 3: (Color online) In 2D spinon Fermi sea case, (a) the scattered dots are temperature T dependence of I_s/T (V the spin bias on the right lead). They can be fitted by simple lines($y \propto x$). (b) The spin current I_s versus spin bias V on the right lead at different temperatures T (fitted by simple lines). The cut point at origin indicates $I_s \propto V$. (a) and (b) together indicate $I_s \propto T^2 V$ at high temperature $k_BT >> V$.

$$H_M = \sum_{\boldsymbol{k}} E_0(a^\dagger_{\boldsymbol{k}} a_{\boldsymbol{k}} + b^\dagger_{\boldsymbol{k}} b_{\boldsymbol{k}} + \gamma_{\boldsymbol{k}} a_{\boldsymbol{k}} b_{-\boldsymbol{k}} + \gamma_{\boldsymbol{k}} a^\dagger_{\boldsymbol{k}} b^\dagger_{-\boldsymbol{k}})$$

where $E_0 = 2ZS|J|$ and $\gamma_{\boldsymbol{k}} = \sum_{\boldsymbol{\delta}} \cos(\boldsymbol{k}\cdot\boldsymbol{\delta})/Z$ with δ sums over the nearest-neighbor lattice sites. Here Z is the coordination number, S is spin quantum number and J is

TABLE I: Behavior of the spin current through the interface between different Mott insulators(rows) and a metallic lead with respect to the spin bias V and temperature T.

	$T=0$	$k_BT >> V$
1-d spinon Fermi sea	$\propto V^3$	$\propto (k_BT)^2V$
2-d spinon Fermi sea	$\propto V^3$	$\propto (k_BT)^2V$
2-d Dirac spin liquid	$\propto V^5$	$\propto (k_BT)^4V$
collinear antiferromagnet	$\propto V\|V\|^3$	$\propto (k_BT)^3V$

TABLE II: Numerical estimates of the induced spin bias in the left lead with different kinds of Mott insulator middle regions(rows) at three different temperatures $T = 0K$, $1K$, and $10K$. Other parameters used are given in the main text.

	$T=0K$	$T=1K$	$T=10K$
1-d spinon Fermi sea	$0.3nV$	$10nV$	$1000nV$
2-d spinon Fermi sea	$0.07nV$	$3nV$	$300nV$
Dirac spin liquid	$2\times10^{-7}nV$	$5\times10^{-4}nV$	$3nV$

the spin exchange constant. $b_{\boldsymbol{k}}$ ($b^\dagger_{\boldsymbol{k}}$) and $a_{\boldsymbol{k}}$ ($a^\dagger_{\boldsymbol{k}}$), are the annihilation (creation) of Holstein-Primakoff bosons[39] on B-sublattice and A-sublattice, respectively.

Since spin wave dispersions is $E_q = 4\sqrt{2}S|J|qa$ with a the lattice constant on square lattice, the density of states of spin excitations is

$$\frac{1}{N_R^2}\sum_{\boldsymbol{q}} A_M(q,\omega) \propto \omega^2.$$

The spin current $I_s \propto V|V|^3$ and $I_s \propto (k_BT)^3V$ at T=0, and $T>0$ with $V << k_BT$, respectively.

All the cases we have discussed above are summarized in Table I.

Numerical estimates of the spin current. We use the following estimates of the parameters[40], with the interface exchange coupling $J_I = 10meV$ and spin bias $V = 1k_B \approx 0.1meV$. The metallic conductivity $\rho = 10^{-8}\Omega\cdot m$, lattice constant $a = 0.3nm$, and Fermi level $E^e_F = 1eV$. The effective spinon mass $m_s \approx 10m_e$ and Fermi level $E^s_F = 10meV$. The bias induced in the left lead is evaluated by $V_L \approx (2e/\hbar)(I_s/N_\perp) * \rho * l_s$ with $N_\perp$ the number of transverse mode (see Table II).

Discussions. Many factors ignored by our analysis may affect the results. First we have assumed the conservation of the z-component of spin in the entire system, so the spin current is well-defined. However in the real materials spin-orbit coupling(SOC) will generically be present[2]. We hope our results can still be applied to such systems if the linear dimensions of the sample are much smaller than the inverse of SOC. For the same reason we did not considered non-collinear AFM orders, e.g. the 120° order on triangular lattice.

Secondly we have ignored the emergent $U(1)$ gauge field in the spinon Fermi sea and Dirac spin liquid cases. It is well-known[41,42] that coupling to this gauge field can significantly change the low energy behaviors of the (spinon) Fermi sea. However such effects have not been found in the specific heat and thermal conductivity measurements of the organic spin liquid candidates, the conventional Fermi liquid behaviors were observed instead[24,27,30]. We therefore believe our results are still valid in these materials. The effect of $U(1)$ gauge field is an interesting theoretical question and will be left for future studies.

Finally we have assumed a clean and free spinon or magnon system in the middle region, without any scattering of spinons or magnons by interactions among themselves or impurites. We think this is not a serious problem for experiments, according to the large value of 1μm of the experimentally estimated spinon mean free path[30].

In summary, we propose to experimentally identify the spinons by measuring the spin current flowing through the spin liquid candidate materials, which would be a direct test for the existence of spin-carrying mobile excitations. By the nonequilibrium Green function technique we evaluate the spin current through the interface between a Mott insulator and a metal under a spin bias. It is found that different kinds of Mott insulators, including quantum spin liquids, can be distinguished by different relations between the spin current spin bias as well as temperature. We hope our results can stimulate more experimental studies of the spin liquid candidate materials and further promote the exchange of ideas between different fields (e.g. spintronics and strongly correlated electrons) in condensed matter physics.

This work was financially supported by MOST of China (2012CB921303, 2009CB929100 and 2012CB821402), NSF-China under Grants Nos. 11074174, 11121063, 91221302 and 11274364.

---

[1] P. W. Anderson, Mater. Res. Bull. **8**, 153 (1973).
[2] L. Balents, Nature (London) **464**, 199 (2010).
[3] P. W. Anderson, Science **235**, 1196 (1987).
[4] P. A. Lee, N. Nagaosa, and X. G. Wen, Rev. Mod. Phys. **78**, 17 (2006).
[5] G. Misguich, B. Bernu, C. Lhuillier, and C. Waldtmann, Phys. Rev. Lett. **81**, 1098 (1998).
[6] M. Q. Weng, D. N. Sheng, Z. Y. Weng, R. J. Bursill, Phys. Rev. B **74**, 012407 (2006).
[7] S. Yunoki, S. Sorella, Phys. Rev. B **74**, 014408 (2006).
[8] D.N. Sheng, O. I. Motrunich, and M.P.A. Fisher, Phys. Rev. B **79**, 205112 (2009).
[9] H.-Y. Yang, A. M. Läuchli, F. Mila, and K. P. Schmidt, Phys. Rev. Lett. **105**, 267204 (2010).
[10] P. Lecheminant, B. Bernu, C. Lhuillier, L. Pierre, and P. Sindzingre, Phys. Rev. B **56**, 2521 (1997).

[11] H.C. Jiang, Z.Y. Weng, and D.N. Sheng, Phys. Rev. Lett. **101**, 117203 (2008).
[12] Simeng Yan, D. A. Huse, and S. R. White, Science **332**, 1173 (2011).
[13] H.-C. Jiang, H. Yao, and L. Balents, Phys. Rev. B **86**, 024424 (2012).
[14] H. Morita, S. Watanabe, and M. Imada, J. Phys. Soc. Jpn. **71**, 2109 (2002).
[15] Z. Y. Meng, T. C. Lang, S. Wessel, F. F. Assaad, and A. Muramatsu, Nature **464**, 847 (2010).
[16] D.J. Klein, J. Phys. A. Math. Gen. **15**, 661 (1982).
[17] A. Kitaev, Ann. Phys. **321**, 2 (2006).
[18] H. Yao, and D.-H. Lee, Phys. Rev. Lett. **107**, 087205 (2011).
[19] P. A. Lee, Science **321**, 1306 (2008).
[20] Y. Shimizu, K. Miyagawa, K. Kanoda, M. Maesato, and G. Saito, Phys. Rev. Lett. **91**, 107001 (2003).
[21] Y. Okamoto, M. Nohara, H. Aruga-Katori, and H. Takagi, Phys. Rev. Lett. **99**, 137207 (2007).
[22] J. S. Helton, K. Matan, M. P. Shores, E. A. Nytko, B. M. Bartlett, Y. Yoshida, Y. Takano, A. Suslov, Y. Qiu, J.-H. Chung, D. G. Nocera, and Y. S. Lee Phys. Rev. Lett. **98**, 107204 (2007).
[23] T. Itou, A. Oyamada, S. Maegawa, M. Tamura, R. Kato, Phys. Rev. B **77**, 104413 (2008).
[24] M. Yamashita, N. Nakata, Y. Kasahara, T. Sasaki, N. Yoneyama, N. Kobayashi, S. Fujimoto, T. Shibauchi, and Y. Matsuda, Nature Phys. **10**, 44 (2008).
[25] F. L. Pratt, P. J. Baker, S. J. Blundell, T. Lancaster, S. Ohira-Kawamura, C. Baines, Y. Shimizu, K. Kanoda, I. Watanabe, G. Saito, Nature (London) **471**, 612 (2011).
[26] S. Yamashita, Y. Nakazawa, M. Oguni, Y. Oshima, H. Nojiri, Y. Shimizu, K. Miyagawa, and K. Kanoda, Nature Phys. **4**, 459 (2008).
[27] S. Yamashita, T. Yamamoto, Y. Nakazawa, M. Tamura, R. Kato, Nature Commun. **2**, 275 (2011).
[28] O. I. Motrunich, Phys. Rev. B **72**, 045105 (2005).
[29] S.-S. Lee and P. A. Lee, Phys. Rev. Lett. **95**, 036403 (2005).
[30] M. Yamashita, N. Nakata, Y. Senshu, M. Nagata, H. M. Yamamoto, R. Kato, T. Shibauchi, and Y. Matsuda, Science **328**, 1246 (2010).
[31] N. Tombros, C. Jozsa, M. Popinciuc, H. T. Jonkman, and B. J. van Wees, Nature (London) **448**, 571 (2007).
[32] D.-K. Wang, Q.-F. Sun, and H. Guo, Phys. Rev. B **69**, 205312 (2004).
[33] H.-Z. Lu and S.-Q. Shen, Phys. Rev. B **77**, 235309 (2008); Q.-F. Sun, Y. Xing, and S.-Q. Shen, *ibid.* **77**, 195313 (2008).
[34] M. R. Norman, and T. Micklitz, Phys. Rev. Lett. **102**, 067204 (2009); P. Bruno, Phys. Rev. B **52**, 411 (1995); M. D. Stiles, *ibid.* **48**, 7238 (1993); **54**, 14679 (1996).
[35] H. Haug and A.-P. Jauho, *Quantum Kinetics in Transport and Optics of Semiconductors*, 2nd ed. (Springer, Berlin, 2008).
[36] Gerald D. Mahan, *Many-Particle Physics* (Plenum Press, New York, 1981).
[37] See supplemental matarial for the derivation of this fact.
[38] Y. Ran, M. Hermele, P. A. Lee, and X.-G. Wen, Phys. Rev. Lett. **98**, 117205 (2007).
[39] T. Holstein, and H. Primakoff, Phys. Rev. **58**, 1908 (1940).
[40] Y. Kajiwara, K. Harii, S. Takahashi, J. Ohe, K. Uchida, M. Mizuguchi, H. Umezawa, H. Kawai, K. Ando, K. Takanashi, S. Maekawa, and E. Saitoh, Nature **464**, 262 (2010).
[41] B. I. Halperin, P. A. Lee, and N. Read, Phys. Rev. B **47**, 7312 (1993).
[42] C. P. Nave, P. A. Lee, Phys. Rev. B **76**, 235124 (2007).

arXiv:1301.1488v2 [cond-mat.str-el] 19 Nov 2013

supplementary material of detect spinons via spin current

Chui-Zhen Chen,[1] Qing-feng Sun,[1] Fa Wang,[2] and X. C. Xie[2]
[1] *Institute of Physics, Chinese Academy of Sciences, Beijing 100190, China*
[2]*International Center for Quantum Materials and School of Physics, Peking University, Beijing 100871, China*

(Dated: December 16, 2013)

I. SPIN CURRENT

In the main text, we have introduced

$$\begin{aligned} I_s = \frac{J_I^2 N_\perp}{4N_R^2 N_M^2} &\sum_{\boldsymbol{q},\boldsymbol{k},\boldsymbol{k'}} A_M(\boldsymbol{q}, \xi_{Rk'\uparrow} - \xi_{Rk\downarrow} + V)\delta_{\boldsymbol{q}_\perp + \boldsymbol{k}_\perp - \boldsymbol{k'}_\perp} \\ &\times\{[1 + n_B(\xi_{Rk'\uparrow} - \xi_{Rk\downarrow} + V)]n_F(-\xi_{Rk\downarrow})n_F(\xi_{Rk'\uparrow}) \\ &-n_B(\xi_{Rk'\uparrow} - \xi_{Rk\downarrow} + V)n_F(\xi_{Rk\downarrow})n_F(-\xi_{Rk'\uparrow})\} \end{aligned} \tag{1}$$

where N_M and N_R is the number of unit cells in the middle region and right lead, respectively. Here $N_\perp$ is the number of transverse mode(parallel to the interface) and $V = \mu_{R\uparrow} - \mu_{R\downarrow}$ is the spin bias in the right lead. $n_B(\omega)$ and $n_F(\xi_{Rk\sigma})$ are the Bose and Fermi distribution function, respectively. $\delta_{\boldsymbol{q}_\perp + \boldsymbol{k}_\perp - \boldsymbol{k'}_\perp}$ indicates transverse(parallel to the interface) momentum conservation. The power spectrums A_M are defined as $A_M(\boldsymbol{q}, \omega) = \int dt < S_M^-(-\boldsymbol{q}, t)S_M^+(\boldsymbol{q}, 0) > \exp(i\omega t)/n_B(\omega)$, where $S_M^\pm(\boldsymbol{q}, t)$ is the Fourier form of $S_M^\pm(\boldsymbol{r}, t) = S_M^x(\boldsymbol{r}, t) \pm S_M^y(\boldsymbol{r}, t)$.

In the main text, we have assumed that the transverse momentum conservation term can be separated properly. This will be explained it in detail in the rest of this material.

II. SPIN LIQUID

We describe gapless spin liquids by the following mean-field Hamiltonian

$$H_M = \sum_{\boldsymbol{k},\sigma} \zeta_k f^\dagger_{\boldsymbol{k}\sigma} f_{\boldsymbol{k}\sigma}$$

where f are fermionic spinons and $\zeta_k = \epsilon_k - \mu_s$ with μ_s the spinon chemical potential. In this case, $\boldsymbol{S}_M(\boldsymbol{r}) = \frac{1}{2}\sum_{\mu,\mu'} \boldsymbol{\sigma}_{\mu\mu'} f^\dagger_\mu(\boldsymbol{r}) f_{\mu'}(\boldsymbol{r})$, with $\boldsymbol{\sigma}$ the Pauli matrix and $\mu =\uparrow, \downarrow$. The spinon dispersion ϵ_k may have a Fermi surface (the "spinon Fermi sea" state[1,2]) or Dirac points at Fermi level[3].

Because

$$\begin{aligned} < S_M^-(-\boldsymbol{q}, t)S_M^+(\boldsymbol{q}, 0) > &= < \sum_{\boldsymbol{p},\boldsymbol{p'}} f^\dagger_{p-q\downarrow}(t) f_{p\uparrow}(t) f^\dagger_{p'+q\uparrow}(0) f_{p'\downarrow}(0) > \\ &= \sum_{\boldsymbol{p}} < f^\dagger_{p-q\downarrow}(t) f_{p-q\downarrow}(0) >< f_{p\uparrow}(t) f^\dagger_{p\uparrow}(0) >, \end{aligned}$$

we get

$$\begin{aligned} &\sum_{\boldsymbol{q}} A_M(\boldsymbol{q}, \omega)\delta_{\boldsymbol{q}_\perp + \boldsymbol{k}_\perp - \boldsymbol{k'}_\perp} \\ &= \sum_{\boldsymbol{q}} \delta_{\boldsymbol{q}_\perp + \boldsymbol{k}_\perp - \boldsymbol{k'}_\perp} \frac{1}{n_B(\omega)} \int dt \exp(i\omega t) < S_M^-(-\boldsymbol{q}, t)S_M^+(\boldsymbol{q}, 0) > \\ &= \sum_{\boldsymbol{q},\boldsymbol{p}} \delta_{\boldsymbol{q}_\perp + \boldsymbol{k}_\perp - \boldsymbol{k'}_\perp} \frac{n_F(\zeta_{p-q})\, n_F(-\zeta_p)\delta(\omega - \zeta_p + \zeta_{p-q})}{n_B(\omega)} \\ &= \sum_{\boldsymbol{p'},\boldsymbol{p}} \delta_{\boldsymbol{p}_\perp - \boldsymbol{p'}_\perp + \boldsymbol{k}_\perp - \boldsymbol{k'}_\perp} \frac{n_F(\zeta_{p'})\, n_F(-\zeta_p)\delta(\omega - \zeta_p + \zeta_{p'})}{n_B(\omega)}. \end{aligned}$$

Now we come to the two dimensional spinon Fermi sea case, which is the most relevant to the 2D organic spin liquid candidate materials. If the energy of spinon excitations ζ_k and spin-↑ (↓) electron excitations $\xi_{Rk\uparrow(\downarrow)}$ are much smaller spinon Fermi level μ_s and spin-↑ (↓) electron Fermi level $\mu_{R\uparrow(\downarrow)}$,

$$\begin{aligned}\boldsymbol{p}_\perp - \boldsymbol{p}'_\perp + \boldsymbol{k}_\perp - \boldsymbol{k}'_\perp &= p\cos\theta_1 - p'\cos\theta'_1 + k\cos\theta_2 - k'\cos\theta'_2 \\ &\approx k^s_F\cos\theta_1 - k^s_F\cos\theta'_1 + k^e_{F\downarrow}\cos\theta_2 - k^e_{F\uparrow}\cos\theta'_2.\end{aligned}$$

In the two dimensional Dirac spin liquid case[3], the low energy spinon dispersion is $\epsilon_q = \pm\hbar v_F|q - q_F|$, with v_F the Fermi velocity and q_F the Fermi vector,

$$\begin{aligned}\boldsymbol{p}_\perp - \boldsymbol{p}'_\perp + \boldsymbol{k}_\perp - \boldsymbol{k}'_\perp &= p\cos\theta_1 - p'\cos\theta'_1 + k\cos\theta_2 - k'\cos\theta'_2 \\ &\approx k^e_{F\downarrow}\cos\theta_2 - k^e_{F\uparrow}\cos\theta'_2.\end{aligned}$$

Since $\boldsymbol{p}_\perp - \boldsymbol{p}'_\perp + \boldsymbol{k}_\perp - \boldsymbol{k}'_\perp$ is the only angular dependent term, we can express the spin current as

$$\begin{aligned}I_s = \frac{J_I^2\Theta_l N_\perp}{4N_R^2N_M^2}&\sum_{\boldsymbol{q},\boldsymbol{k},\boldsymbol{k}'} A_M(\boldsymbol{q}, \xi_{Rk'\uparrow} - \xi_{Rk\downarrow} + V) \\ &\times\{[1 + n_B(\xi_{Rk'\uparrow} - \xi_{Rk\downarrow} + V)]n_F(-\xi_{Rk\downarrow})n_F(\xi_{Rk'\uparrow}) \\ &-n_B(\xi_{Rk'\uparrow} - \xi_{Rk\downarrow} + V)n_F(\xi_{Rk\downarrow})n_F(-\xi_{Rk'\uparrow})\}, \end{aligned} \tag{2}$$

with $\Theta_l = \int d\theta_1 d\theta'_1 d\theta_2 d\theta'_2(\cos\theta_1 - \cos\theta'_1 + k^e_{F\downarrow}/k^s_F\cos\theta_2 - k^e_{F\uparrow}/k^s_F\cos\theta'_2)/(2\pi)^4$ for spinon Fermi sea case and $\Theta_l = \int d\theta_2 d\theta'_2(\cos\theta_2 - k^e_{F\uparrow}/k^e_{F\downarrow}\cos\theta'_2)/(2\pi)^4$ for U(1) Dirac spin liquid, respectively.

Thus the transverse momentum conservation term is separated independently.

We note that in one dimension case, $\Theta_l = 1$ and the number transverse mode $N_\perp = 1$.

III. COLLINEAR ANTIFERROMAGNETIC NÉEL ORDER.

Let us now consider the simplest AFM ordered state, the collinear AFM Néel order on a bipartite lattice, and show that it has different spin transport behavior compared to the previous spin liquid cases. We describe the spin excitations by a linearized spin wave Hamiltonian,

$$H_M = \sum_{\boldsymbol{k}} E_0(a^\dagger_{\boldsymbol{k}}a_{\boldsymbol{k}} + b^\dagger_{\boldsymbol{k}}b_{\boldsymbol{k}} + \gamma_{\boldsymbol{k}}a_{\boldsymbol{k}}b_{-\boldsymbol{k}} + \gamma_{\boldsymbol{k}}a^\dagger_{\boldsymbol{k}}b^\dagger_{-\boldsymbol{k}})$$

where $E_0 = 2ZS|J|$ and $\gamma_{\boldsymbol{k}} = \frac{1}{Z}\sum_\delta\cos(\boldsymbol{k}\cdot\boldsymbol{\delta})$ with δ sums over the nearest-neighbor lattice sites. Here Z is the coordination number, S is spin quantum number and J is the spin exchange constant. In this case, $S^+_M(\boldsymbol{r}) = S^x_M(\boldsymbol{r}) + iS^y_M(\boldsymbol{r}) = a^\dagger(\boldsymbol{r}) + b(\boldsymbol{r})$, $S^-_M(\boldsymbol{r}) = S^x_M(\boldsymbol{r}) - iS^y_M(\boldsymbol{r}) = a(\boldsymbol{r}) + b^\dagger(\boldsymbol{r})$ and $S^z_M(\boldsymbol{r}) = a^\dagger(\boldsymbol{r})a(\boldsymbol{r}) - b^\dagger(\boldsymbol{r})b(\boldsymbol{r})$, where $a(\boldsymbol{r})$ $[a^\dagger(\boldsymbol{r})]$ and $b(\boldsymbol{r})$ $[b^\dagger(\boldsymbol{r})]$ are the Fourier form of $a(\boldsymbol{k})$ $[a^\dagger(\boldsymbol{k})]$ and $b(\boldsymbol{k})$ $[b^\dagger(\boldsymbol{k})]$, respectively. Here, $b_{\boldsymbol{k}}$ $(b^\dagger_{\boldsymbol{k}})$ and $a_{\boldsymbol{k}}$ $(a^\dagger_{\boldsymbol{k}})$ are the annihilation (creation) of Holstein-Primakoff bosons[4] on B-sublattice and A-sublattice, respectively.

If the wave vector of spin wave is much smaller than spin-↑ (↓) electron Fermi vector, i.e. $k_1 << k^e_{F\uparrow}(k^e_{F\downarrow})$,

$$\boldsymbol{q}_\perp - \boldsymbol{k}_\perp + \boldsymbol{k}'_\perp = q\cos\theta_1 - k\cos\theta_2 + k'\cos\theta_3 \approx k^e_{F\downarrow}\cos\theta_2 - k^e_{F\uparrow}\cos\theta_3.$$

The spin current is

$$\begin{aligned}I_s = \frac{J_I^2\Theta_w N_\perp}{4N_R^2N_M^2}&\sum_{\boldsymbol{q},\boldsymbol{k},\boldsymbol{k}'} A_M(\boldsymbol{q}, \xi_{Rk'\uparrow} - \xi_{Rk\downarrow} + V) \\ &\times\{[1 + n_B(\xi_{Rk'\uparrow} - \xi_{Rk\downarrow} + V)]n_F(-\xi_{Rk\downarrow})n_F(\xi_{Rk'\uparrow}) \\ &-n_B(\xi_{Rk'\uparrow} - \xi_{Rk\downarrow} + V)n_F(\xi_{Rk\downarrow})n_F(-\xi_{Rk'\uparrow})\}, \end{aligned} \tag{3}$$

with $\Theta_w = \int d\theta_2 d\theta_3\delta(\cos\theta_2 - k^e_{F\uparrow}/k^e_{F\downarrow}\cos\theta_3)/(2\pi)^3$. Thus the transverse momentum conservation term is separated.

---

[1] O. I. Motrunich, Phys. Rev. B **72**, 045105 (2005).

[2] S-S. Lee and P. A. Lee, Phys. Rev. Lett. **95**, 036403 (2005).

[3] Y. Ran, M. Hermele, P. A. Lee, and X.-G. Wen, Phys. Rev. Lett. **98**, 117205 (2007).

[4] T. Holstein, and H. Primakoff, Phys. Rev. **58**, 1908 (1940).